Safanah M. Raafat
Department of Control and System Engineering, University of Technology Baghdad, Iraq.
60154@uotechnology.edu.iq

Zainab SH. Mahmoud
Department of Control and System Engineering, University of Technology, Baghdad, Iraq.
zainabalsafar299@gmail.com

Received on: 07/01/2018
Accepted on: 08/11/2018
Published online: 25/12/2018

Robust Multiple Model Adaptive Control for Dynamic Positioning of Quadrotor Helicopter System

Abstract- *The quadrotor control has been one of the benchmark control problems. It is considered as an under-actuated, multivariable and high nonlinear system due to its dynamics, having strong coupling between translation and angular motion and affected by external disturbances associated with flight environment. Therefore, there is a need to design a robust control that can keep up with sudden changes and find better tracking performance against modeling error and uncertainties. In this work, an adaptive state feedback control method denoted as Classical Multiple Model Adaptive Control (CMMAC) has been implemented. This method embodies in its structure a bank of filters. Kalman filter (KF) has been used where each filter has been designed for a specific value of an equilibrium point and set of controllers, which was provided by the LQ-servo design. Comparisons of the performance of a quadrotor system between control designs for single Kalman filter with CMMAC for the same value of uncertainty in terms of Root Mean Square Error (RMSE) have been presented. CMMAC meets better performance of tracking design for all variations; the performance of the controlled quadrotor has been improved for the linear and angular coordinates 100%, as compared to the performance when using one Kalman filter.*

Keywords- *quadrotor, Kalman filter, Classical Multiple Model Adaptive control (CMMAC), LQ-servo control, tracking performance, performance indices.*

How to cite this article: S.M. Raafat, and Z.SH. Mahmoud, "Robust Multiple Model Adaptive Control for Dynamic Positioning of Quadrotor Helicopter System," *Engineering and Technology Journal*, Vol. 36, Part A, No. 12, pp. 1249-1259, 2018.

1. Introduction

Nowadays, the development of technologies makes the study of micro Unmanned Air Vehicles (UAVs) very interesting. UAV means an aircraft which can fly without a pilot. UAVs have gained a great importance at present, because they have usefulness in a variety of areas, for an instance, conducting research in hazardous and large-scale fields [1]. Quadrotor belongs to the rotary UAVs type and it is characterized by the simplicity in construction, ease of maintenance and less complicated in dynamics compared to a helicopter [2]. Micro quadrotor UAVs are small in size and have lightweight components. These features make the systems very sensitive to any variation and external disturbance uncertainty. As a result, additional payload, uncertainty in aerodynamic and gyroscopic coupling may change quadrotor dynamics dramatically affecting the stability and tracking response of the system. This problem raises the need for a robust control in order to meet a better tracking performance. In addition to the need for the estimation of the unmeasured variables required for controller design [3].

Many types of strategies and methods have been implemented for controlling a quadrotor, some of them for stabilizing quadrotor attitudes as, [4-9], others for controlling a full quadrotor states as [10-16]. For such a system, the controller design should be advanced, to alleviate any disturbances and adaptive to attains stabilizing and tracking in the presence of uncertainties. Therefore, the application of model-based control methods may not be adequate since they cannot satisfy completely stabilization of the system due to the uncertainty in the dynamics of a quadrotor. An adaptive method that based on a set of controllers designed for a reference model will be a competitive approach.

The Adaptive Multiple Model (AMM) is a methodology that is based on linear model implementation in real time. It can efficiently deal with large sets of uncertainties. The Multiple Model approach has been explained by references [17,18]. It consists of a set of controllers and an identification module. A bank of filters is used for identification module which can achieve an optimal value for the estimated output, or a performance index for calculating a feedback control law [19].

https://doi.org/10.30684/etj.36.12A.6
2412-0758/University of Technology-Iraq, Baghdad, Iraq

Many applications employed the Multiple Model Method (MMM) as: The authors in [20] achieved the trajectory design of 2DOF robotic manipulators. The continuous dynamic positioning systems had been designed for ships and offshore rigs subjected to the influence of sea waves in [21]. Reference [22] diagnosed the error in micro electro mechanical system/ Lateral Comb Resonators**.** In reference [23], the authors had suggested MMM to improve the existing collision avoidance systems of vehicles for different scenarios like cured path and using the data from Global Positioning System (GPS). In[24]**,** the authors designed a procedure for F-8C aircraft to control longitudinal and lateral dynamics under several altitudes, air speed, and level of turbulence**.** In this work, Classical Multiple Mode Adaptive Control (CMMAC) is used to meet stability and performance requirement of tracking for a reference model. This will be achieved by selecting an appropriate control signal correlated with highest probability. Each Kalman filter is designed for a model corresponding to each known value of the uncertain parameter. A cost function Root Mean Square Error (RMSE) of the adaptive control has used to determine the error between actual response and references [19,25].

This paper is organized as follow: Section 2 presents the dynamics model of a Draganflyer IV quadrotor which derived by using Newton Euler formulation. Section 3 and section 4 present the continuous time Kalman filter and LQ-servo, respectively. CMMAC is explained in section 5 and its performance and simulation result of tracking design are drawn in section 6 for a reference model.

2. The Quadrotor Model

I. Definitions

A quadrotor is a rotary wing UAV composing of four identical rotors with propeller sets on motors, all located at the ends of a plus structure or configuration**.** Two distinct coordinate systems will be used when the quadrotor is moving in three dimensional spaces in order to define position and orientation. One is the body coordinate system, the other is the navigation frame (inertial frame), were forces have an effect. The quadrotor build based on some assumption [26]:

- Quadrotor is modeled as a plus configuration with four rotors.
- Quadrotor propeller frame of rotation is assumed fixed and parallel and blades are of fixed pitch so a quadrotor structure is a rigid body and the derivation of a rigid- body dynamics can be performed by applying Newton's second law and Euler's rotational equation of motion.
- The quadrotor configuration is symmetrical over its center of gravity which makes the matrix of moment of inertia a diagonal matrix which has the same value on x-axis and y-axis and the off-diagonal elements can be omitted.
- Center of gravity and body axis origin are similar.
- Euler angular rate and body angular rate are the same near hovering.

The quadrotor is rotated on its axes with an angular velocity. This angular velocity is represented as ***p, q*** and ***r*** corresponding to x-axis, y-axis and z-axis, respectively, the two frames set direction to north, east and down and follow right hand rule, $[x\ y\ z]$ is a navigation coordinate frame, $[x_b\ y_b\ z_b]$ is the body coordinate frame as shown in Figure 1. Quadrotor position represents by $\boldsymbol{P^n} = [x\ y\ z]$ and the velocity of quadrotor is represented in body coordinate frame, indexed *'V':* $\boldsymbol{V^B} = [p\ q\ r]^T$, the rotation of quadrotor is described by Euler angles, where the three Euler angles which are denoted by roll ϕ, pitch Θ, and ψ respectively [27]. The desired orientation is achieved by rotating three times around body coordinate frame. The total transformation from body frame to navigation frame is achieve by the three matrixes will be multiplied together; the resulting is a rotation matrix, indexed 'R_B^I' [28].

$$R_B^I = \begin{bmatrix} C\psi C\Theta & C\psi S\Theta S\phi - S\psi C\phi & C\phi S\Theta C\psi + S\phi S\psi \\ S\psi C\Theta & S\psi S\Theta S\phi + C\psi C\phi & C\phi S\Theta S\psi - S\phi C\psi \\ -S\Theta & C\Theta S\phi & C\phi C\Theta \end{bmatrix} \quad (1)$$

From assumption, the propeller has fixed-pitch blades and propellers axes of rotation are fixed. So that the speed is the only changing variable of the propellers [28]. The opposite blades are matched and rotate in the same direction [29], so the motors M_1 and M_3 rotate in the clockwise direction when seeing from above, while motors M_2 and M_4 rotate in the counterclockwise direction. The angular velocities of the motors are written $\boldsymbol{w} = [\mathrm{w}_1\ \mathrm{w}_2\ \mathrm{w}_3\ \mathrm{w}_4\ ]^{\mathrm{T}}$.

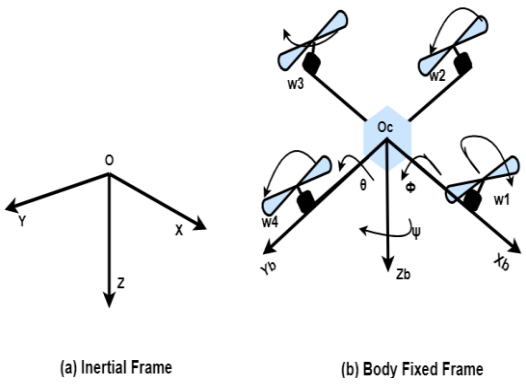

Figure 1: Navigation frame and body frame [29].

II. Quadrotor kinematics

The kinematics of the quadrotor is represented as the movement of the craft body as one piece within the surroundings environment with no information that specifies the force and moments that really generate these movements. The velocity of the quadrotor is calculated from a time derivative for position data. The linear velocity of the craft will be related by rotation matrix as demonstrated in the Equation below [2]:

$$\begin{bmatrix}\dot{x}\\ \dot{y}\\ \dot{z}\end{bmatrix}_{inertial}\begin{bmatrix}(C\psi C\Theta)\dot{x}_{Body}+\\ (S\psi C\Theta)\dot{x}_{Body}+\\ (-S\Theta)\dot{x}_{Body}+\\ (C\psi S\Theta S\phi - S\psi C\phi)\dot{y}_{Body}+(C\phi S\Theta C\psi + S\phi S\psi)\dot{z}_{Body}\\ (S\psi S\Theta S\phi + C\psi C\phi)\dot{y}_{Body}+(C\phi S\Theta S\psi - S\phi C\psi)\dot{z}_{Body}\\ (C\Theta S\phi)\,\dot{y}\_Body+(C\phi C\Theta)\dot{z}\_Body\end{bmatrix} \quad (2)$$

where *S ( )* and *C ( )* represent sine and cosine, respectively, the linear velocity in navigation frame comes from the inverse of the rotation matrix multiplied by a linear velocity in body coordinate frame. All attitude angles are changing with time, so the relationship between the Euler angles rates in navigation system with the body angular rates with regard to the body fixed system are calculated by using the transformation matrix. At the beginning, the navigation attitude rates and the body attitude rates seem to be one and the same. The Euler rate depends on the angular displacement of the navigation systems. Equation (3) illustrates the Euler angle rates related to the body axis rates [8].

$$\begin{bmatrix}\dot{\phi}\\ \dot{\Theta}\\ \dot{\psi}\end{bmatrix}_{inertial}=\begin{bmatrix}1 & S\phi t\Theta & C\phi t\Theta\\ 0 & C\phi & -S\phi\\ 0 & S\phi sec\Theta & C\phi sec\Theta\end{bmatrix}\begin{bmatrix}p\\ q\\ r\end{bmatrix}_{Body} \quad (3)$$

III. Quadrotor Dynamics

The dynamics describe behavior of quadrotor which is characterized by under-actuated and coupled system. The vehicle has six degrees of freedom (three degrees for translation and three degrees for angles about a translation axes) and only four control inputs. The under-actuated state means that there are two states which are uncontrollable and couple [28]. In this case, *x* and *y* positions are coupled and depended on the angles of rotation with regard to control inputs. The dynamic model is represented by understanding and determining various forces and moments applied to generate accurate model and generate equation of motion by using Newton-Euler formalism which is written by Eq.(4) [30]:

$$\begin{bmatrix}F^B\\ \tau\end{bmatrix}=\begin{bmatrix}m\times I & 0_{3\times3}\\ 0_{3\times3} & I_{x,y,z}\end{bmatrix}\begin{bmatrix}\dot{V}^B\\ \dot{\omega}^B\end{bmatrix}+\begin{bmatrix}\omega^B\times(m\,V^B)\\ \omega^B\times(I_{x,y,z}\,\omega^B)\end{bmatrix} \quad (4)$$

The variable m represents the mass in (*Kg*), $\boldsymbol{I}$ is the identity matrix, $\boldsymbol{I_{x,y,z}}$ is a moment of inertia in (x-axis, y-axis, and z-axis) and V^B, ω^B represent linear and angular velocity of the system. The total force represent on the quadrotor are the sum of forces shown in advance:

$$F^B_{tot}=F^B_{gBody}-F^B_{thrust}+F^B_{drag}+F^B_{disturbances}$$
$$=m\times\dot{V}^B+\omega^B x\,(m\,V^B) \quad (5)$$

$$F^B_{tot}=\begin{bmatrix}m\,\ddot{x}^B\\ m\,\ddot{y}^B\\ m\,\ddot{z}^B\end{bmatrix}+\begin{bmatrix}\dot{\Theta}\dot{z}-\dot{\psi}\dot{y}\\ \dot{\psi}\dot{x}-\dot{x}\dot{z}\\ \dot{\phi}\dot{y}-\dot{\Theta}\dot{x}\end{bmatrix}$$
$$=m_{tot}\times\begin{bmatrix}-g\times S\Theta\\ g\times C\Theta S\phi\\ g\times C\phi C\Theta\end{bmatrix}-\begin{bmatrix}0\\ 0\\ b\times(w_1^2+w_2^2+w_3^2+w_4^2)\end{bmatrix} \quad (6)$$

The forces on the quadrotor create moments in the different axes. The moment generally has the following:

$$\tau=I_{xyz}\,\dot{\omega}^B+\omega^B\times(I_{xyz}\,\omega^B) \quad (7)$$

In a model the thrust forces and length from center of gravity to the center of the propeller cause moment in the three axes:

$$\tau_{thrust}=\begin{bmatrix}\tau x\\ \tau y\\ \tau z\end{bmatrix}=\begin{bmatrix}l\times(F_4-F_2)\\ l\times(F_3-F_1)\\ T_1+T_2+T_3+T_4\end{bmatrix}$$
$$=I_{xyz}\,\dot{\omega}^B+\omega^B\times(I_{xyz}\,\omega^B) \quad (8)$$

$$\text{where}\begin{bmatrix}l\times(F_4-F_2)\\ l\times(F_3-F_1)\\ T_1+T_2+T_3+T_4\end{bmatrix}=\begin{bmatrix}u_2\\ u_3\\ u_4\end{bmatrix} \quad (9)$$

$$\begin{bmatrix}u_2\\ u_3\\ u_4\end{bmatrix}=\begin{bmatrix}I_{xx}\times\ddot{\phi}^B\\ I_{yy}\times\ddot{\Theta}^B\\ I_{zz}\times\ddot{\psi}^B\end{bmatrix}+[(\dot{\phi}i+\dot{\Theta}j+\dot{\psi}k)\times\begin{pmatrix}Ixx\,\dot{\phi}\,i\\ Iyy\,\dot{\Theta}\,j\\ Izz\,\dot{\psi}k\end{pmatrix}] \quad (10)$$

where F^B_{drag} and $F^B_{disturbances}$ are neglected in the model. Coriolis terms are picked up when the linear velocities are crossed (vector product) with the angular velocities and T_1, T_2, T_3, T_4 are drug

moments have the relationship with thrust force on each arm.

IV. Equations of motion

Equations of motion for quadrotor system which have been derived above can be represented as in Eq. (11) and Eq. (12) [28]:

$$\begin{bmatrix}\ddot{x}^B\\ \ddot{y}^B\\ \ddot{z}^B\end{bmatrix}=\begin{bmatrix}-g\times S\Theta\\ g\times C\Theta S\phi\\ g\times C\phi C\Theta\end{bmatrix}-\frac{1}{m}\begin{bmatrix}0\\0\\b\times(w_1^2+w_2^2+w_3^2+w_4^2)\end{bmatrix} \quad (11)$$

$$\begin{bmatrix}\ddot{\phi}^B\\ \ddot{\Theta}^B\\ \ddot{\psi}^B\end{bmatrix}=\begin{bmatrix}u_2/I_{xx}\\ u_3/I_{yy}\\ u_4/I_{zz}\end{bmatrix}+\begin{bmatrix}\dot{\Theta}\dot{\psi}(I_{zz}-I_{yy})/I_{xx}\\ \dot{\phi}\dot{\psi}(I_{xx}-I_{zz})/I_{yy}\\ \dot{\Theta}\dot{\phi}(I_{yy}-I_{xx})/I_{zz}\end{bmatrix} \quad (12)$$

The movement of the quadrotor results from the processing of the thrust force and drag moment prepared by the four rotors. The thrust force and drug moment have the relationship with rotors speed as given in the following equations [30]:

$$F=b\times \boldsymbol{w}^2 \quad (13)$$

$$T=d\times \boldsymbol{w}^2 \quad (14)$$

Equations (13) and (14) represent the effect of angular velocity of the motors. The thrust force and moments are considered as control inputs

$$F_{thrust}(\boldsymbol{w}^2)=(w_1^2+w_2^2+w_3^2+w_4^2)\times b=u_1 \quad (15)$$

$$\boldsymbol{\tau}_{\phi}(w_{2,4})=(w_4^2-w_2^2)\times b\times l=u_2 \quad (16)$$

$$\tau_{\Theta}(w_{1,3})=(w_1^2-w_3^2)\times b\times l=u_3 \quad (17)$$

$$\boldsymbol{\tau}_{\psi}(\boldsymbol{w})=(w_2^2+w_4^2-w_1^2-w_3^2)\times d=u_4 \quad (18)$$

The states of the craft are the linear location, linear velocities, Euler angles and angular velocities. These 12 state variables form the state vector of the quadrotor and these provided in Eq. (19)

$$\boldsymbol{x}=\begin{bmatrix}x & \dot{x} & y & \dot{y} & z & \dot{z} & \phi & \dot{\phi} & \Theta & \dot{\Theta} & \psi & \dot{\psi}\end{bmatrix}^{\boldsymbol{T}} \quad (19)$$

These states form the equation of motion in body coordinate system. The Body Fixed Frame (BFF) and Inertial Frame (IF) are related. Accordingly, these states can be made in IF as:

$$\dot{\boldsymbol{x}}=f(\boldsymbol{x},u) \quad (20)$$

$$\begin{bmatrix}\dot{\boldsymbol{x}}\\ \ddot{\boldsymbol{x}}\\ \dot{\boldsymbol{y}}\\ \ddot{\boldsymbol{y}}\\ \dot{\boldsymbol{z}}\\ \ddot{\boldsymbol{z}}\\ \dot{\boldsymbol{\phi}}\\ \ddot{\boldsymbol{\phi}}\\ \dot{\Theta}\\ \ddot{\Theta}\\ \dot{\boldsymbol{\psi}}\\ \ddot{\boldsymbol{\psi}}\end{bmatrix}=\begin{bmatrix}\boldsymbol{x}_2\\ \frac{-(cos\phi\ sin\Theta\ cos\psi+sin\phi\ sin\psi)\times F_{thrust}}{m}\\ \boldsymbol{x}_4\\ \frac{-(cos\phi\ sin\Theta\ cos\psi-sin\phi\ cos\psi)\times F_{thrust}}{m}\\ \boldsymbol{x}_6\\ g-(\frac{(cos\phi\ cos\Theta)\times F_{thrust}}{m}\\ \boldsymbol{x}_8\\ \dot{\Theta}\dot{\psi}(I_{zz}-I_{yy})/I_{xx}+\tau_{\phi}/I_{xx}\\ \boldsymbol{x}_{10}\\ \dot{\phi}\dot{\psi}(I_{xx}-I_{zz})/I_{yy}+\tau_{\Theta}/I_{yy}\\ \boldsymbol{x}_{12}\\ \dot{\Theta}\dot{\phi}(I_{yy}-I_{xx})/I_{zz}+\tau_{\psi}/I_{zz}\end{bmatrix} \quad (21)$$

Equation (21) displays twelve state variables effectively controlled from the rotational rate of the motors. In this work, it is needed to put the model in a matrix format for a linear control. This was proved by linearizing the equations of motion at any operating point, as explains in Eq. (22), when the vehicle is in a hovering situation. While the vehicle is hovering, the angles roll and pitch should be stabilized so that there would be no movement in x and y position because they are coupled. The positions *x* and *y*, altitude *z*, and the rotation angle *yaw* could be a constant. In this work, the assumed operating point is written below in Eq. (23) and the control input signals of linear model at the operating point are explained in Eq. (24).

$$\boldsymbol{x_{eq}}=[x,0,y,0,z,0,0,0,0,0,\psi,0] \quad (22)$$

$$\boldsymbol{x_{eq}}=\boldsymbol{x_{op}}=[0\ 0\ 0\ 0-8\ 0\ 0\ 0\ 0\ 0\ 0\ 0] \quad (23)$$

$$u_{eq}=[u_1,u_2,u_3,u_4] \quad (24)$$

where $\boldsymbol{x_{eq}}$ and u_{eq} are the equilibrium point and the control signal for a linearized quadrotor at hovering situation. For hovering situation the control signal $u_1=F_{thrust}=mg$ and the other u_2, u_3 and u_4 are zeros. The state space format of the equations of motion at any equilibrium point is:

$$\dot{\boldsymbol{x}}=A\,\boldsymbol{x}+Bu \quad (25)$$

$$y=C\,\boldsymbol{x} \quad (26)$$

where $A=\frac{df}{d\boldsymbol{x}}\Big|_{\boldsymbol{x}=\boldsymbol{x_{eq}}}$, $B=\frac{df}{du}\Big|_{u=u_{eq}}$

$$A = \begin{bmatrix} 0 & 1 & 0 & 0 & 0 & 0 & 0 & 0 & 0 & 0 & 0 & 0 \\ 0 & 0 & 0 & 0 & 0 & 0 & 0 & 0 & -g & 0 & 0 & 0 \\ 0 & 0 & 0 & 1 & 0 & 0 & 0 & 0 & 0 & 0 & 0 & 0 \\ 0 & 0 & 0 & 0 & 0 & 0 & g & 0 & 0 & 0 & 0 & 0 \\ 0 & 0 & 0 & 0 & 0 & 1 & 0 & 0 & 0 & 0 & 0 & 0 \\ 0 & 0 & 0 & 0 & 0 & 0 & 0 & 0 & 0 & 0 & 0 & 0 \\ 0 & 0 & 0 & 0 & 0 & 0 & 0 & 1 & 0 & 0 & 0 & 0 \\ 0 & 0 & 0 & 0 & 0 & 0 & 0 & 0 & 0 & 0 & 0 & 0 \\ 0 & 0 & 0 & 0 & 0 & 0 & 0 & 0 & 0 & 1 & 0 & 0 \\ 0 & 0 & 0 & 0 & 0 & 0 & 0 & 0 & 0 & 0 & 0 & 0 \\ 0 & 0 & 0 & 0 & 0 & 0 & 0 & 0 & 0 & 0 & 0 & 1 \\ 0 & 0 & 0 & 0 & 0 & 0 & 0 & 0 & 0 & 0 & 0 & 0 \end{bmatrix} \quad (27)$$

$$B = \begin{bmatrix} 0 & 0 & 0 & 0 \\ 0 & 0 & 0 & 0 \\ 0 & 0 & 0 & 0 \\ 0 & 0 & 0 & 0 \\ -1/m & 0 & 0 & 0 \\ 0 & 0 & 0 & 0 \\ 0 & 1/I_{xx} & 0 & 0 \\ 0 & 0 & 0 & 0 \\ 0 & 0 & 1/I_{yy} & 0 \\ 0 & 0 & 0 & 0 \\ 0 & 0 & 0 & 1/I_{zz} \\ 0 & 0 & 0 & 0 \end{bmatrix} \quad (28)$$

$$C = \begin{bmatrix} 1 & 0 & 0 & 0 & 0 & 0 & 0 & 0 & 0 & 0 & 0 & 0 \\ 0 & 0 & 1 & 0 & 0 & 0 & 0 & 0 & 0 & 0 & 0 & 0 \\ 0 & 0 & 0 & 0 & 1 & 0 & 0 & 0 & 0 & 0 & 0 & 0 \\ 0 & 0 & 0 & 0 & 0 & 0 & 1 & 0 & 0 & 0 & 0 & 0 \\ 0 & 0 & 0 & 0 & 0 & 0 & 0 & 0 & 1 & 0 & 0 & 0 \\ 0 & 0 & 0 & 0 & 0 & 0 & 0 & 0 & 0 & 0 & 1 & 0 \end{bmatrix} \quad (29)$$

where g is the gravitational acceleration and the adopted parameters for Draganfler IV have been used in Eqs. (27) to (29) [28].

3. Continuous Time Kalman Filter

The main limitation of many control methods is based on the fact that all-state variables of any system are assumed to be measured. Whilst in practical field/reality, it is usually difficult to measure all of these state variables because measuring all states will be with a high cost [31]. Besides, the measurement can never be exact. These issues provide a great importance of estimation methods that can estimate physical state variables of a process more easily from available measurements. The Kalman Filter (KF) is a powerful linear estimator, which generates an optimal state estimate for a linear system, subjected to the assumptions listed below:

1. Noise Statistics: Both the process noise ζ and measurement noise M are zero mean, white noise sequences whose properties are described below;

$$E[\zeta(t)\,] = 0 \quad (30)$$

$$E[M(t)\,] = 0 \quad (31)$$

$$E[\zeta(t)\,\zeta(t)'\,] = Q \quad (32)$$

$$E[M(t)\,M(t)'\,] = R \quad (33)$$

2. Initial States: The initial states vector is a random variable which has the properties below;

Mean**:**

$$E[\boldsymbol{x}(\mathbf{0})] = \boldsymbol{x_o} \quad (34)$$

and

Variance**:**

$$E[(\boldsymbol{x} - \hat{\boldsymbol{x}})(\boldsymbol{x} - \hat{\boldsymbol{x}})^{\boldsymbol{T}}] = \boldsymbol{s_O} \quad (35)$$

3. System Parameters: The parameters of $\boldsymbol{A}$, $\boldsymbol{B}$ and $\boldsymbol{C}$ are defined in Eqs. (27) to (29). The optimality represents the minimum estimation error covariance. The function of a filter is to eliminate the noisy effects in a signal or information [32, 33].

One of the important functions of the KF here is that its gain still improves until a steady state situation is reached where no further improvement is obtained. Also, the assumed noise strength in the internal model of filters is based on the information obtained from available measurement, so the filter continues to be tuned as much as possible. This algorithm is often called adaptive or self-tuning estimation algorithm. The key for adaptation is the residual signal of the estimator as it can be seen in Figure 2. It represents the difference between the actual measurement and estimated measurement from the filter's model, a consistent mismatch means an error exists in a formulated model, and this mismatch provided the need for adaptation.

The steady-state KF model can be described by the following set of differential equations [34]:

$$\dot{x}(t) = A(t)\,x(t) + B(t)\,u(t) + \zeta(t) \quad (36)$$

$$y(t) = C(t)\,x(t) + M(t) \quad (37)$$

Here $x(t)$ is the state vector, $u(t)$ is the control signal,A is a system matrix, B is an input matrix applied to control signal, C is the measurement matrix, $y(t)$ is the measurement noise vector and the measurements noise $M(t)$ have Gaussian distribution.

The KF is described by the following Eqs. (38) to (41);

$$\dot{\hat{x}} = A\,\hat{x} + Bu + L\,(y - C\,\hat{x}) \quad (38)$$

$$\hat{y} = C\,\hat{x} \quad (39)$$

$$\dot{s} = A^T\,s + sA - sBR^{-1}\,B^T\,s + Q \quad (40)$$

$$L = s\,C^T\,R^{-1} \quad (41)$$

where [*A*, *B*] are assumed to be controllable, the symmetric positive definite weighting matrices $\boldsymbol{\zeta}$ and *M* are viewed as tuning parameters that, both matrices are taken as relative to each other, and assuming that the precise characteristics of the noises are not known.

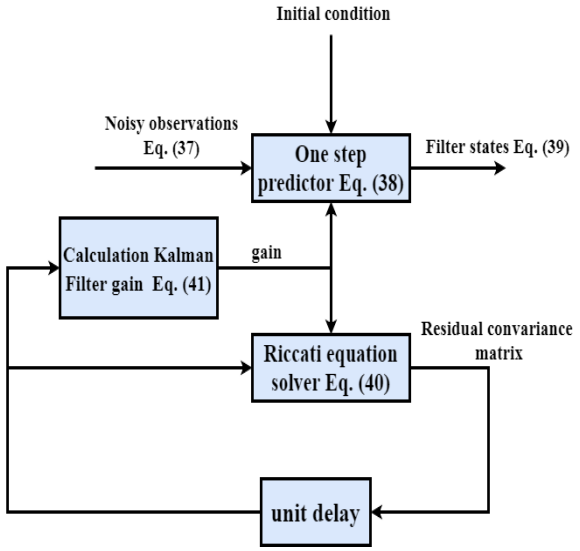

Figure 2: Kalman filter algorithm.

4. Linear Quadratic (LQ)-Servo Optimal Control

Traditional LQR is an optimal control method which guarantees stability and brings states to zero [35] whilst the LQ - servo controller is another kind of state feedback optimal control which can provide tracking the dynamic reference and eliminate the error due to the absence of an integral term in this controller. A designated system of LQ-control, which is shown in Figure 3, includes the output states of the LQR control as a part of the state variable and the integral of error vector (four states) to improve the tracking performance [13]. Let the error be ***e,*** the state space of the including error vector can be written as follows:

$$\dot{e} = r - y = r - Cx_{(6\times1)} \quad (42)$$

where ***r*** is the reference signals of linear and angular positions and the state space of the designated system written as follows:

$$\dot{x}_E = A_E\,x_E + B_E\,u \quad (43)$$

$$\begin{bmatrix}\dot{x}\\ \dot{e}\end{bmatrix} = \begin{bmatrix}A & 0\\ -C & 0\end{bmatrix}\begin{bmatrix}x\\ e\end{bmatrix} + \begin{bmatrix}B\\ 0\end{bmatrix} \times u + \begin{bmatrix}0\\ I\end{bmatrix} \times r \quad (44)$$

where the x_E, K_E, A_E and B_E represent the augmented of state vectors, control gains, system matrix, input matrix, respectively, where A_E and B_E must be controllable [36].
From the augmented system representation, the control input matrix u is calculated by:

$$x_I = [\int(x_r - x) \quad \int(y_r - y) \quad \int(z_r - z) \quad \int(\psi_r - \psi)\,]^T \quad (45)$$

$$x_E = [x \quad \dot{x} \quad y \quad \dot{y} \quad z \quad \dot{z} \quad \phi \quad \dot{\phi} \quad \theta \quad \dot{\theta} \quad \psi \quad \dot{\psi} \quad x_I]^T \quad (46)$$

$$u = -K_E \times x_E \quad (47)$$

where K_E is calculated in MATLAB from linear model matrices by using ***lqr*** command.

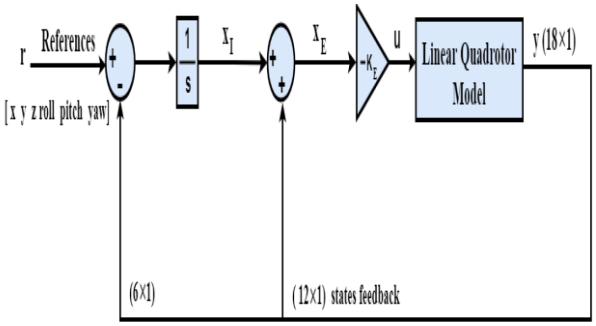

Figure 3: State feedback structure of LQ-servo controller.

5. Continuous Time-Classical Multiple Model Adaptive Controller (CT-CMMAC)

In flying environment, the quadrotor is exposed to uncertainties that may cause variations in the plant's parameters as a result of mechanical wear, friction coefficients increase, or due to changes in operational circumstances [37]. So these variations and uncertainties lead to performance degradation or instability.
Assume that the plant model states $\boldsymbol{x}$ is subjected to parameter uncertainty (*a*), then the linear plant is represented as follows; the plant is time invariant, multiple-input-multiple-output (MIMO) subject to ξ and *M* noise signals, respectively:

$$\dot{\boldsymbol{x}}(t) = A_a\, \boldsymbol{x}(t) + B_a\ u(t) + \ G_a\, \zeta(t) \qquad (48)$$

$$y(t) = C_a\, \boldsymbol{x}(t) + M(t) \qquad (49)$$

The MMAC consists of: i) *N* weighting signal, p_N, from a dynamic generator weighting signals and ii) a bank of N continuous-time estimators, KF_N, where each estimator is designed based on one of the selected models adopted. Notice that these selected models are chosen from the original set of the plant model.

The vector of uncertain parameters is represented in the linear state model for a dynamic system; these parameters change the matrices which define the structure of the linear model. For tractable representation, it is assumed that (a)can take only one value for each run.

The dynamic weights represent the best guess about which models are likely enough to be correct. They are considered as the key in Multiple Model algorithm and they are calculated online. The initial value of dynamic weighting at time zero is equal to *I/N* and satisfy the following condition, that

$$(\ p_i(t)) \ \in \ (0,1) \qquad \textit{For i=1-N} \qquad (50)$$

The dynamic weights are created by a differential equation named Dynamic Weighting Signal Generator (DWSG) which is represented as follows [25]:

$$\dot{P}_i(t) = -£\left(1 - \frac{\beta_i(t)\ e^{-w_i\,(t)}}{\sum_{j=1}^{N} P_j\,(t)\ \beta_j(t)\ e^{-w_j\,(t)}}\right) P_i(t) \qquad (51)$$

£ is a positive constant, $\beta_{\ i}(t)$ is a function, and $w_i(t)$ is an error measuring continuous function that relates the measurement states of the plant and the estimated measurable states of each local estimator to a nonnegative real value. These functions are calculated, respectively as follows [25]:

$$w_i(t) = \frac{1}{2}\|y(t) - \hat{y}_i(t)\|_2\ S_i^{-1}(t) \qquad (52)$$

$$\beta_i(t) = \frac{1}{\sqrt{det\, S_i(t)}} \qquad (53)$$

$$S_i = \mathrm{C\ s_i\ C^T} + \mathrm{R}_i \qquad (54)$$

where s_i is a uniformly positive definite weighting matrix which is already calculated in Eq. (40) , R_i is a variance of noisy measurement vector , $y(t)$ is noisy measurement vector calculated in Eq. (37), $\hat{y}_i(t)$ is an estimated measurement from the filter's model at the selected value of uncertainty and

$$\|x\|_2 S = (x^T S\ x\ )\ \hat{}\ (1/2) \qquad (55)$$

Each control signal is produced from the product of the state estimation of the $KF\ \hat{x}_{\ k}(t|t), k = 1,2,..N$, and the gain associated with optimal linear quadratic control; G_k; is given by [25, 38]

$$u_k(t) = -G_k\ \hat{x}_k(t|t), k = 1,2,\ldots\ldots N \qquad (56)$$

N is equal to 3 in this paper. The 'global' control signal u(*t*), which inters to both of the plant and the banks of KFs , is computed by the probabilistic weighting of each local control signal [25, 38].

Finally, the mixing between the state estimation and feedback control generation can be clearly noticed; any errors in the estimation of the state will directly have an effect on the local control signals. So, in the CT-CMMAC architecture, there is no separation-principle of an identification system and a control system [39], as shown in Figure 4.

6. Simulation Results

The application of CT-CMMAC for changing the operating point will be illustrated. From the state space matrices of the linear model, which have been explained in Section 2 in Eqs. (27), (28) and (29). The value of sample time is 0.001 sec. The CT-CMMAC built employs three Kalman Filters as shown in Figure 4. The(a) value equals to 0, 0.78, and 1.2 *rad* for Kalman Filter number 1, 2, and 3, respectively. Three filters are run in parallel when the parameter (a) is assigned to the reference model. For each case, the filters are initialized with $\boldsymbol{x_o} = [2\ 0\ 3\ 0 - 10\ 0\ 0.2\ 0.3\ 0\ 0.7]$ set to the current $\boldsymbol{x}$ values, and the initial weighting signal is uniformly distributed $\boldsymbol{P_o}$*= 1/3*. Figure 5 shows the time histories of the conditional probabilities for these three cases. The system tracks the references in about 15 sec. This illustrates the ability of the algorithm to identify constant parameters with relatively rapid convergence. The close loop responses of CMMAC and residual signal of three filters has been represented when the model and filter start at the same initial point. Figure 6 shows the response of the linear position $\boldsymbol{x}$ by using CMMAC, where (curve 1) represents the actual response from the model, the estimated signal represented in (curve 2) and the reference signal is explained in (curve 3). The Figures 7, 8 and 9 also show the tracking for y and z position, roll, pitch, and yaw,

respectively. Figure 10 shows the time histories for the residual signal from the three filters when yaw position is 0.78 *rad*, so the correct control signal is provided by KF_2 and the related probability goes to one.

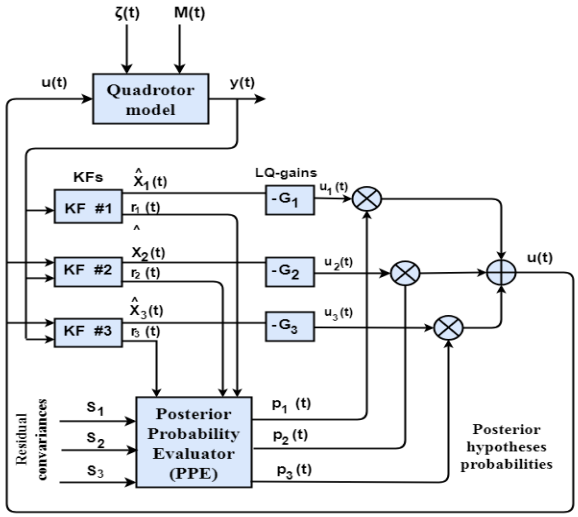

Figure 4: Block diagram of CMMAC [17]

As can be seen from figures, the linear and angular positions track the references, and the adaptation (intelligence) of this algorithm can be seen clearly in Figures 6, 7, 8 and 9, where the actual response follow the true value by adjusting its parameter (a). Figures 11 and 12 demonstrate the performance of the controller to follow the references for the model which demonstrates the capability of the controller to select the correct control signal. The performance of the adaptive control has been evaluated using the index (RMSE) for the CMMAC, where the value of cost function has been computed for tracking in the same initial point. These results are summarized in Table 1 below. The results of the MMAC are compared with that estimator (where yaw=0.78*rad*). The same initial conditions are used in both cases and the results are summarized in Table 1. The table clearly shows the ability of the CMMAC to track the references better compared to Kalman Filter alone.

From Figures 6-11, a number of observations can be made:

1. The best performance was for the linear position, since the error response is small. The figures clearly show the ability of the CMMAC to track the references significantly better as compared to KF alone.
2. CMMAC always determines the correct control signals.
3. MMAC has a featured advantage on only one KF in that its structure takes into account the possible uncertainty in the model.

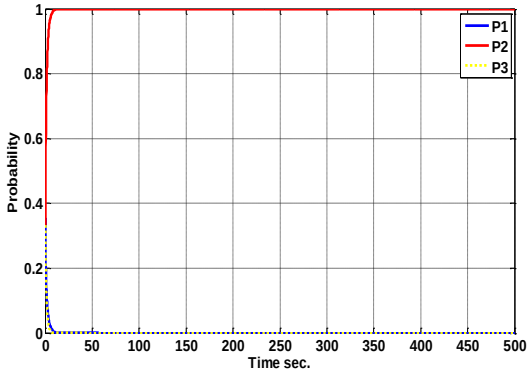

Figure 5: Time histories for probability when the angular velocity yaws=0.78 *rad*.

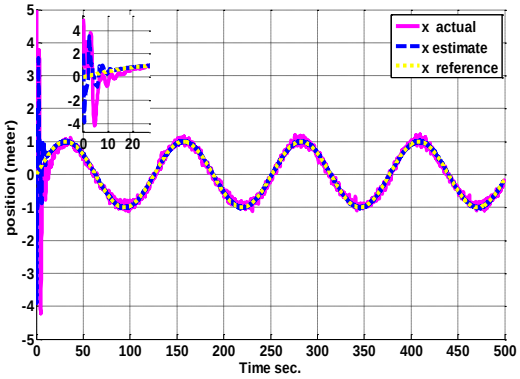

Figure 6: Closed loop response of the linear position x from CMMAC with KF starting at an operating point where yaw=0.78 *rad*.

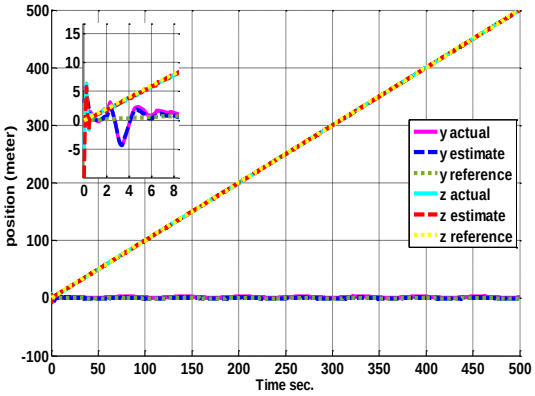

Figure 7: Closed loop response of the linear positions y and z from CMMAC with KF starting at an operating point where yaw=0.78 *rad*.

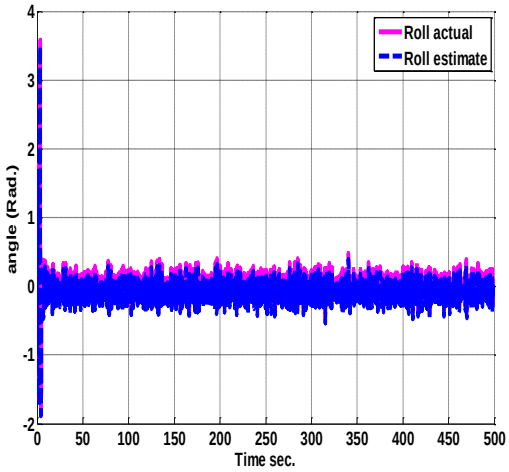

Figure 8: Closed loop response of the position Roll from CMMAC with KF starting at an operating point where yaw=0.78 *rad*.

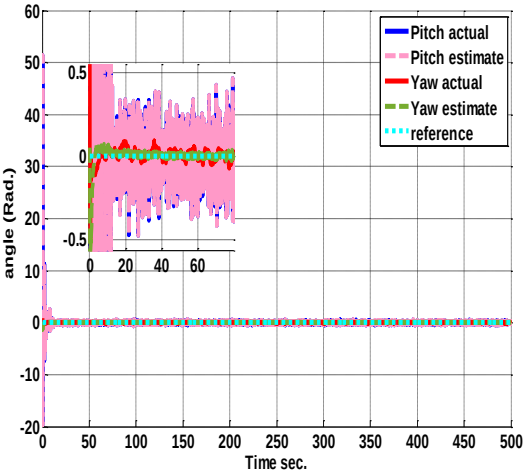

Figure 9: Closed loop response of the positions of Pitch and Yaw from CMMAC with KF starting at an operating point where yaw=0.78 *rad*.

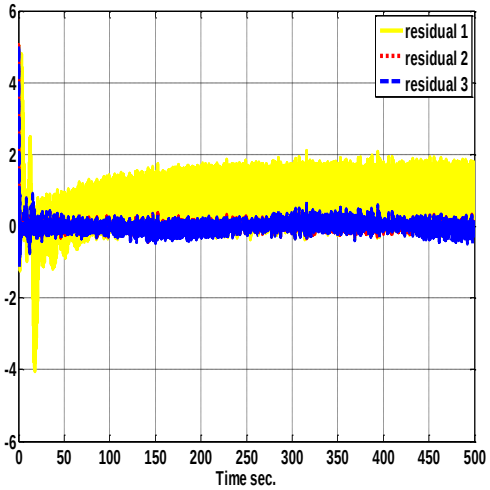

Figure 10: Residual signals when the yaw position in reference model is 0.78 *rad*.

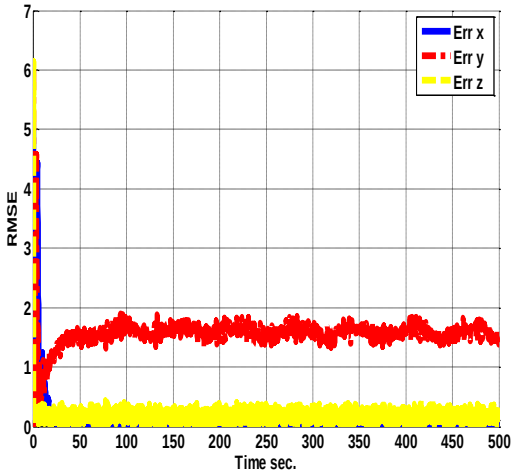

Figure 11: RMSE of the linear position when the yaw position in reference model is 0.78 *rad*.

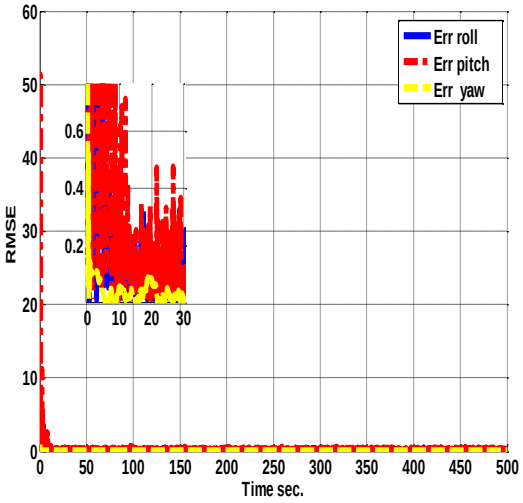

Figure 12: RMSE of the angular position when the yaw position in reference model is 0.78 *rad*.

Table 1: Errors in states by using RMSE between CMMAC and KF when operating at yaw=0.78rad

Quadrotor's states	RMSE for CMMAC	RMSE for KF_2 alone
x	0.1250	unstable
y	0.1541	unstable
z	0.3074	unstable
roll	1.0620	unstable
pitch	0.8868	unstable
yaw	0.0169	unstable

7. Conclusion and Future Work

In this paper, the fundamentals of quadrotor dynamics were studied and the mathematical equation of nonlinear model was derived using Newton-Euler Formula. Then, a linearized model was obtained for an operational point, enabling the linear model to be used in linear control techniques. Also, this paper has presented one of the important problems, which is the stability of the controllers applied to the linearized real system, which is not ensured due to uncertainties. One way of augmenting the stability bounds of the linear model is provided by the adaptive multiple model technique CMMAC. This technique achieves improved tracking performance for a wider range of linear region within yaw position 0-1.5 *rad*. Improvements in tracking performance of 100% in linear and angular position, have been achieved, as compared with using a single KF. Robust performance in presence of uncertainty has been achieved as well. For future work, an intelligent method like fuzzy controller can be examined instead of probability equation to make a better selection of the most suitable plant model for estimation. Moreover, investigate the application of Baram proximity measure for adaptively selecting the nearest nominal value to the actual one.

References

[1] L.R. Newcome, "Unmanned Aviation: A Brief History of Unmanned Aerial Vehicles," American Institute of Aeronautics and astronautics, Inc., (1st Ed.), Reston, Virginia, 1930.

[2] M. D. Schmidt, "Simulation and Control of a Quadrotor Unmanned Aerial Vehicle," M.Sc. Thesis, Electrical Dept. Eng., Univ. of Kentucky, Lexington, Kentucky, USA, 2011.

[3] D. Mellinger, M. Shomin, and V. Kumar, "Control of Quadrotors for Robust Perching and Landing," Int. Powered Lift Conf., Philadelphia, Pennsylvania, USA, pp. 205-225, 2010.

[4] F.A. Al-Saedi and R.A. Sabar, "Design and Implementation of Autopilot System for Quadcopter," *Int. Journal of Science, Engineering and Computer Technology*, Vol.5, No. 6, pp. 190-199, 2015. Available:

http://www.ijcset.net/docs/Volumes/volume5issue6/ijcset2015050613.pdf

[5] D. Yacine, K. Madjid, and A. Aimad, "Fully Decentralized Fuzzy Sliding Mode Control with Chattering Elimination for a Quadrotor Attitude," IEEE, 4th Int. Conf. on Electrical Eng., Boumerdes, Algeria, pp. 1-6, 2015.

[6] E. Abbasi, M. Mahjoob and R. Yazdanpanah, "Controlling of Quadrotor UAV Using a Fuzzy System for Tuning the PID Gains in Hovering Mode," 10th Int. Conf. Adv. Comput. Entertain. Technol., Boekelo, Netherlands, pp. 1-6, 2013.

[7] P. Pounds, R. Mahony, and P. Corke, "Modeling and Control of a Large Quadrotor Robot," *Control Engineering Practice* Sci. [Online], Vol. 18, No.7, pp. 691-699, 2010. Available:

https://www.sciencedirect.com/science/article/pii/S0967066110000456

[8] I.C. Dikmen, A. Arisoy, and H. Temeltas, "Attitude Control of a Quadrotor," IEEE, 4th Int. Conf. on Recent Advances in Space Technologies, RAST'09, Istanbul, Turkey, pp. 722-727, 2009.

[9] S. Bouabdallah, A. Noth, and R. Siegwart, "PID vs LQ Control Techniques Applied to an Indoor Micro Quadrotor," IEEE/RSJ, Int. Conf. on Intelligent Robots and Systems, IROS, Sendal, Japan, pp. 2451-2456, 2004.

[10] M. Moness and M. Bakr, "Development and Analysis of Linear Model Representations of the Quadrotor System," 16th Int. Conf. on Aerospace Siences & Aviation Technology, Cairo, Egypt, 2015.

[11] A.E. EL-Henawy, A.N. Oda, S.A. kader, Quadcopter System Modeling and Autopilot Synthesis, Int. Journal of Engineering Research & Technology, (IJERT) [Online], Vol. 3, No. 1, 2014. Available:

http://citeseerx.ist.psu.edu/viewdoc/download?doi=10.1.1.674.2696&rep=rep1&type=pdf

[12] I. Sadeghzadeh, M. Abdolhosseini and Y. Zhang, "Payload Drop Application Using an Unmanned Quadrotor Helicopter Based on Gain-Scheduled PID and Model Predictive Control," *Unmanned Systems- World Scientific* Sci. [Online], Vol. 2, No. 1, pp. 39-52, 2014. Available: http://sci-hub.tw/https://www.worldscientific.com/doi/pdf/10.1142/S2301385014500034

[13] O. Araar and N. Aouf, "Full Linear Control of a Quadrotor UAV, LQ vs H_∞," IEEE, UKACC Int. Conf. on Control (CONTROL), Loughborough, UK, pp. 133-138, 2014.

[14] H. Bergkvist, "Quadcopter Control Using Android Based Sensing," M.Sc. Thesis, Dept. of Automatic Control, Univ. of Lund, Lund, Sweden, 2013.

[15] L. M. Argentim, W.C. Rezende, P.E. Santos and R.A. Aguiar, "PID, LQR and LQR-PID on a Quadcopter Platform," IEEE, Int. Conf. on Informatics, Electronics & Vision, ICIEV, Dhaka, Bangladesh, pp. 1-6, 2013.

[16] E. Balasubramanian and R. Vasantharaj, "Dynamic Modeling and Control of Quad Rotor, *Int. Journal of Engineering & Technology," (IJET)* [Online], Vol. 5, No. 1, pp. 63-69, 2013. Available:

http://www.enggjournals.com/ijet/docs/IJET13-05-01-013.pdf

[17] S. Fekri, M. Athans and A. Pascoal, "Issues, Progress and New Results in Robust Adaptive Control," *Int. Journal of Adaptive Control & Signal Processing* [Online], Vol. 20, No.10, pp. 519-579, 2006. Available:

http://citeseerx.ist.psu.edu/viewdoc/download?doi=10.1.1.118.9616&rep=rep1&type=pdf

[18] M.G. Safonov, and T.C. Tsao, "The Unfalsified Control Concept and Learning," IEEE, 33rd IEEE Conf. on Decision & Control, Lake Buena Vista, FL, USA, Vol. 3, pp. 2819-2824, 1994.

[19] V. Hassani, J.P. Hespanha, M. Athans and A.M. Pascoal," Stability Analysis of Robust Multiple Model Adaptive Control," *IFAC Proc*. [Online], Vol. 44, No. 1, pp. 350-355, 2011.

[20] J. Hao, G. Tao, and T. Rugthum, "A dynamic Prediction Error Based Adaptive Multiple-Model Control Scheme for Robotic Manipulators," IEEE, American Control Conf., ACC, Seattle, WA, USA, pp. 1791-1796, 2017.

[21] V. Hassani, A.J. Sørensen, A.M. Pascoal, and A.P. Aguiar, "Multiple Model Adaptive Wave Filtering For Dynamic Positioning of Marine Vessels," IEEE, American Control Conf., ACC, Montreal, QC, Canada, pp. 6222-6228, 2012.

[22] A. Izadian and P. Famouri, "Fault Diagnosis of MEMS Lateral Comb Resonators Using Multiple-Model Adaptive Estimators," *IEEE Trans. on Control Systems Technology* [Online], Vol. 18, No. 5, pp. 1233-1240, 2010.

[23] C. Barrios, H. Himberg, Y. Motai and A. Sad, "Multiple Model Framework of Adaptive Extended Kalman Filtering for Predicting Vehicle Location," IEEE, Intelligent Transportation Systems Conf., ITSC'06., Toronto, Ont., Canada, pp. 1053-1059, 2006.

[24] M. Athans, D. Castanon, K.P. Dunn, C. Greene, W. Lee, N. Sandell, and A. Willsky, "The Stochastic Control of the F-8C Aircraft Using a Multiple Model Adaptive Control (MMAC) Method--Part I: Equilibrium Flight, *"IEEE Trans. on Automatic Control* [Online], Vol. 22, No. 5, PP. 768-780, 1977.

[25] V. Hassani, A.P. Aguiar, A.M. Pascoal, and M. Athans, "Further Results on Plant Parameter Identification Using Continuous-Time Multiple-Model Adaptive Estimators," 48th IEEE Conf. on Decision & Control, held jointly with the 28th Chinese Control Conf., CDC/CCC, Toronto, Ont., Canada, pp. 7261-7266, 2009.

[26] T.L. Wong, R.R. Khan and D. Lee, "Model Linearization and H_{∞}, Controller Design for a Quadrotor Unmanned Air Vehicle: Simulation study," IEEE, 13th International Conf. on Control Automation Robotics & Vision, ICARCV, Singapore, pp. 1490-1495, 2014.

[27] O. Magnussen, and K.E. Skjonhaug, "Modeling, Design and Experimental Study for a Quadcopter System Construction," M.Sc. Thesis, Dept. of Eng., Faculty of Technology and Science, Univ. of Agder, Kristiansand and Grimstad, Norway, 2011.

[28] R. Tesfaye, "Modeling and Control of a Quad-rotor Unmanned Aerial Vehicle at Hovering Position," Electrical Eng., Addis Ababa University, Addis Ababa, Ethiopia, 2012.

[29] B.S.M. Henriques, "Estimation and Control of a Quadrotor Attitude," Ph.D. Thesis, Technical Univ. of Lisbon, Lisbon, Portugal, 2011.

[30] J. Li, and Y. Li, "Dynamic Analysis and PID Control for a Quadrotor," IEEE, Int. Conf. on Mechatronics & Automation, ICMA, Beijing, China, pp. 573-578, 2011.

[31] J.B. Burl, "Linear Optimal Control," Addison-Wesley Menlo park, Technique Note, 1999. http://www.me.utexas.edu/~longoria/ssec/leks/Burl_Ch8_LQG.pdf. Visited on 1 January 2018.

[32] O.F. AL-Kubasi, "Development of PC-Based Induction Furnace Thermal Processor," M.Sc. Thesis, Electrical Dept. Eng., Univ. of Technology, Baghdad, Iraq, 2001.

[33] S.M. Raafat, State Estimation of Synchronous PM Motor Drive based on pole Assignment, *Engineering and Technology Journal* [Online], Vol.6, No.1, pp. 20-29, 2006. Available:

https://www.iasj.net/iasj?func=fulltext&aId=69514

[34] M.S. Grewal, Kalman Filtering, (2nd ed.), 2011. Available:

https://wp.kntu.ac.ir/ghaffari/Advanced%20Control-II-2017/Kalman%20Filtering.pdf

[35] B.F. Midhat, "Optimal LQR Controller Design for Wing Rock Motion Control in Delta wing Aircraft," *Engineering and Technology Journal* [Online], Vol. 35, Part A. No. 5, pp. 473-478, 2017. Available:

https://www.iasj.net/iasj?func=fulltext&aId=130206

[36] J. Bae, J. Choi, J. Kim, C. Kim, and J. Yoo, "Two-Wheeled Self-Balancing Robot Based On LQ-Servo with Reduced Order Observer," Fourth Int. Conf. on Information Science & Industrial Applications, ISI, Busan, South Korea, p. 6-9, 2015.

[37] S. Islam, P.X. Liu and A. El Saddik, "Robust Control of Four-Rotor Unmanned Aerial Vehicle with Disturbance Uncertainty," *IEEE Trans. on Industrial Electronics* [Online], Vol. 62, No. 3, pp. 1563-1571, 2015.

[38] A.P. Aguiar, V. Hassani, A.M. Pascoal and M. Athans, "Identification and Convergence Analysis of a Class of Continuous-Time Multiple-Model Adaptive Estimators," *IFAC Proc.* [Online], Vol. 41, No. 2, pp. 8605-8610, 2008. Available:
https://pdfs.semanticscholar.org/b2ee/44a8c37644c0f055aa21efec4401635b5faf.pdf

[39] S. Fekri, M. Athans and A. Pascoal, "Robust Multiple Model Adaptive Control (RMMAC): A case Study," *Int. Journal of Adaptive Control & Signal Processing* [Online], Vol. 21, No.1, pp. 1-30, 2007. Available:

http://citeseerx.ist.psu.edu/viewdoc/download?doi=10.1.1.116.2339&rep=rep1&type=pdf